

Supplementary data

A protease cascade regulates release of the human malaria parasite *Plasmodium falciparum* from host red blood cells

James A Thomas^{1,6}, Michele S Y Tan^{1,6}, Claudine Bisson², Aaron Borg³, Trishant R Umrekar², Fiona Hackett¹, Victoria L Hale^{2§}, Gema Vizcay-Barrena⁴, Roland A Fleck⁴, Ambrosius P Snijders³, Helen R Saibil² and Michael J Blackman^{1,5*}

¹Malaria Biochemistry Laboratory, The Francis Crick Institute, 1 Midland Rd, London NW1 1AT, UK

²Crystallography, Institute of Structural and Molecular Biology, Birkbeck College, London, WC1E 7HX, UK

³Protein Analysis and Proteomics Platform, The Francis Crick Institute, 1 Midland Rd, London NW1 1AT, UK

⁴Centre for Ultrastructural Imaging, Kings College London, London, SE1 9RT, UK

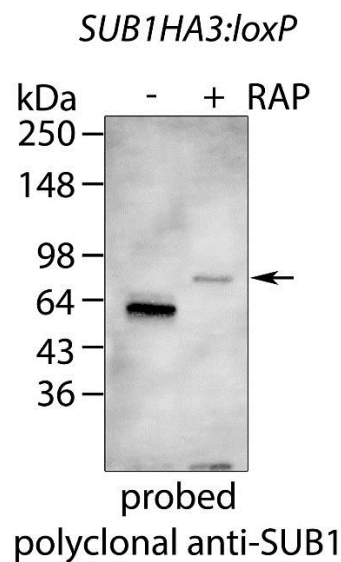
⁵Faculty of Infectious and Tropical Diseases, London School of Hygiene & Tropical Medicine, London, WC1E 7HT, UK

⁶These authors contributed equally

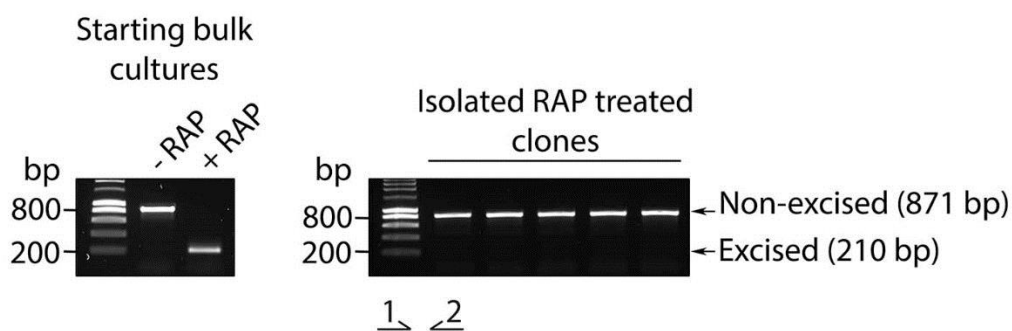
[§]Current address: MRC Laboratory of Molecular Biology, Cambridge Biomedical Campus, Francis Crick Ave, Cambridge CB2 0QH, UK

*e-mail: mike.blackman@crick.ac.uk

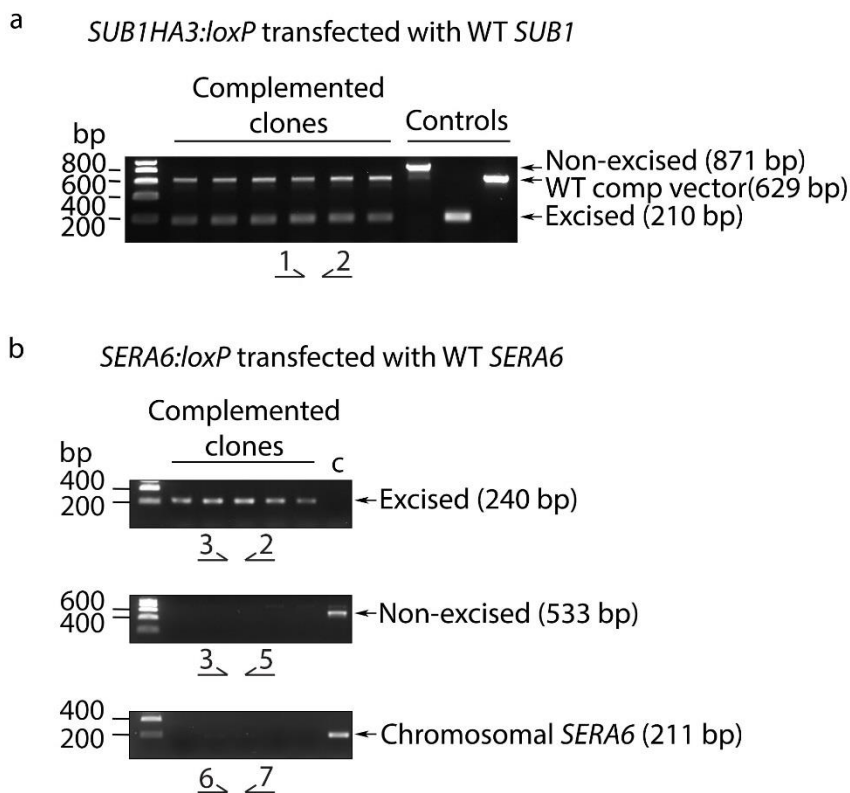
Supplementary Figure 1. Conditional disruption of SUB1 expression. Western blot showing expression of SUB1 in *SUB1HA3:loxP* schizonts ~44 h following treatment of synchronous ring-stage parasites with rapamycin (RAP) to induce gene disruption (+RAP), or mock treatment (-RAP). Schizont extracts were probed with a polyclonal antiserum specific for the catalytic domain of SUB1¹. The major signal in the control -RAP lane corresponds to the accumulated mature form of SUB1 (p47) that results from proteolytic maturation during trafficking to exonemes². The faint signal in the +RAP lane (arrowed) likely represents truncated full-length SUB1 that has not undergone maturation due to the removal of key catalytic residues (see Fig. 1 of the main manuscript). Blot taken from a single experiment.



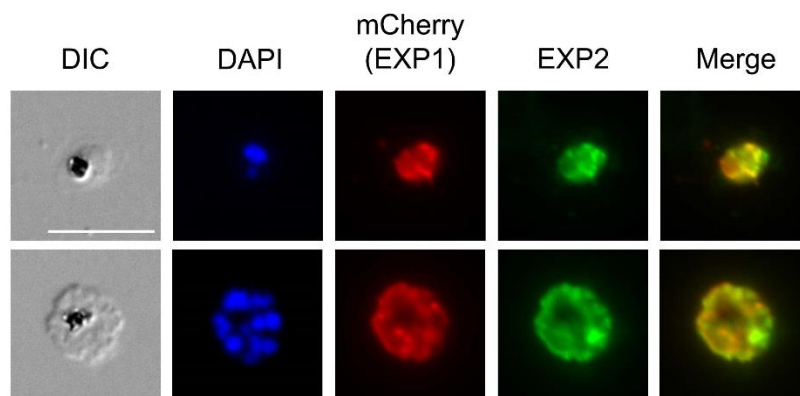
Supplementary Figure 2. Disruption of the *SUB1* gene is lethal. Diagnostic PCR analysis of the *SUB1HA3:loxP* population immediately following RAP-treatment (+RAP) or mock treatment (-RAP) and before plaque assay (Starting bulk cultures), or of parasite clones expanded from plaques produced by the RAP-treated sample. RAP-treatment significantly reduced the PCR signal diagnostic of the intact (non-excised) *SUB1* locus in the starting parasite population and resulted in appearance of a signal diagnostic of the excised locus. In contrast, parasites rescued from plaques produced by the RAP-treated parasites displayed a non-excised genomic architecture, indicating that only the minor population of non-excised parasites were capable of growth. Primers used for PCR analysis are indicated (see [Supplementary Table 1](#) for primer sequences), as are expected sizes of the PCR amplicons. Data taken from a single experiment.



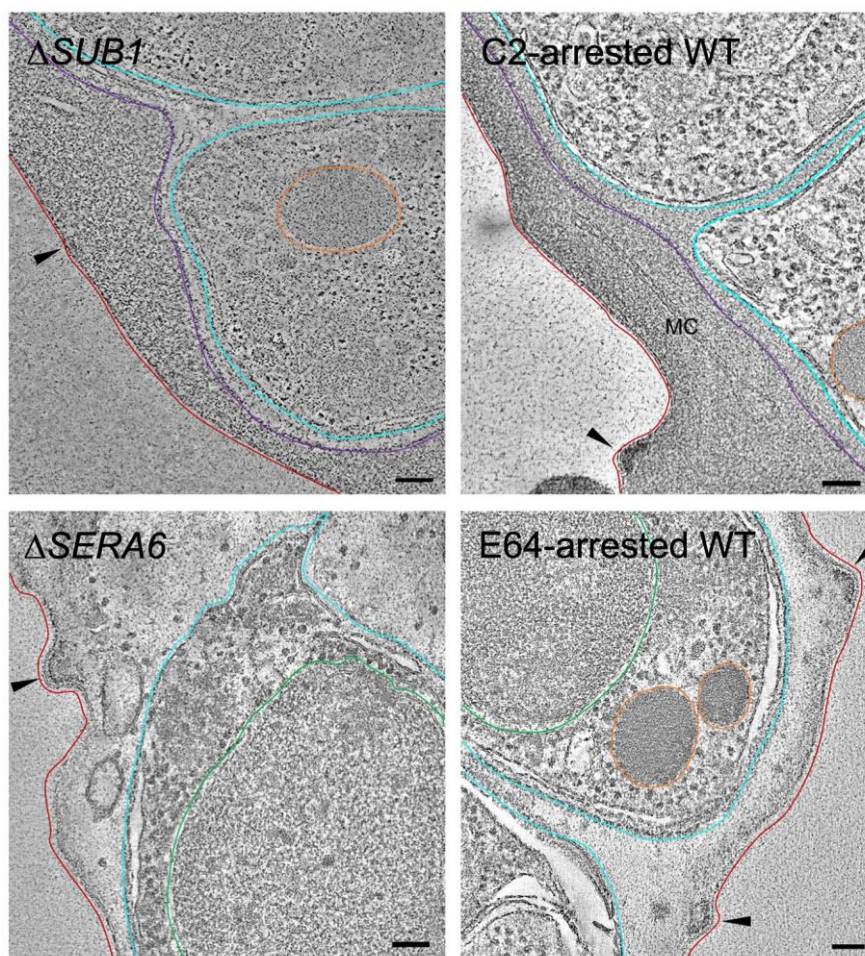
Supplementary Figure 3. Viability of Δ *SUB1* and Δ *SERA6* parasites requires genetic complementation by the respective wild-type gene. Diagnostic PCR analysis of parasite clones (Complemented clones) obtained by expansion of individual wells containing plaques selected following RAP-treatment of: **a**, *SUB1HA3:loxP* parasites transfected with the WT *SUB1* expression vector (6 independent clones); or **b**, *SERA6:loxP* parasites transfected with the WT *SERA6* expression vector (5 independent clones). Identities of primer pairs used for each set of PCR reactions are indicated (see Fig. 1 of the main manuscript for positions of hybridisation of primers, and Supplementary Table 1 for primer sequences). All isolated parasite clones examined were found to possess the respective complementing plasmid and displayed a genomic architecture consistent with excision of the floxed genomic sequence. No viable excised clones were identified that did not harbour the complementing plasmid. Control tracks (labelled 'C' in panel **b**) show the sizes of the indicated amplicons from mock-treated *SUB1HA3:loxP* parasites or complementing WT *SUB1* vector only (**a**), or from mock-treated *SERA6:loxP* parasites (**b**). All data derived from a single experiment in each case.



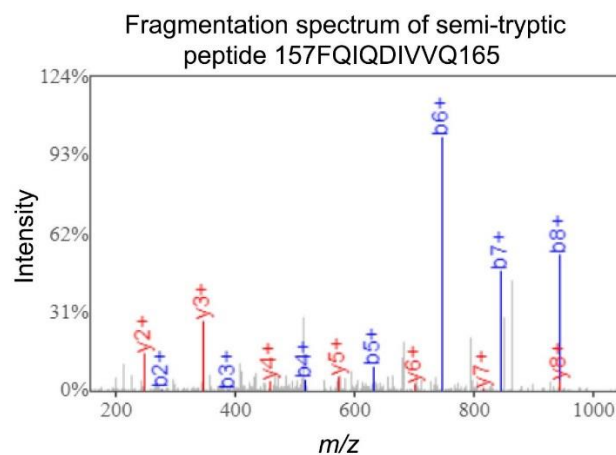
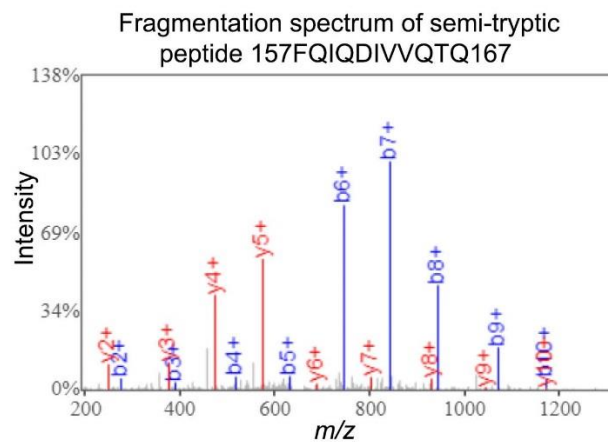
Supplementary Figure 4. Fluorescent labelling of the *P. falciparum* parasitophorous vacuole membrane (PVM). Indirect immunofluorescence analysis of the *SERA6:loxP* parasite line transfected with plasmid pDC2-EXP1-mCherry for constitutive expression of the parasitophorous vacuole membrane (PVM) protein EXP1 fused to mCherry. Shown are a uninuclear trophozoite (top) and a multinucleated schizont stage (bottom) parasite probed with the anti-mCherry polyclonal antibody ab167453 (Abcam) as well as monoclonal antibody 7.7 (<http://www.malariaresearch.eu/>) specific for the distinct endogenous PVM protein EXP2 (PlasmoDB ID PF3D7_1471100). The signals closely overlap, consistent with correct trafficking of the transgenic EXP1mCherry fusion protein to the PVM. DAPI, 4,6-diamidino-2-phenylindole. Scale bar, 10 μm . All data shown are from a single experiment.



Supplementary Figure 5. Electron tomography shows that the Δ *SUB1* phenotype is indistinguishable from arrest by compound 2 (C2), whilst the Δ *SERA6* phenotype mimics inhibition of egress by the cysteine protease inhibitor E64. Each image is an average of 20 slices from a dual-axis tomogram of high-pressure frozen, freeze substituted segmented schizonts. In both the top panels the PVM (highlighted in purple) is intact, surrounding the mature merozoites, whilst in both lower panels the PVM has ruptured and the majority of the surrounding haemoglobin has leaked out, probably due to poration of the red blood cell membrane (RBCM). Knobs identifying the bounding RBCM are indicated (black arrow heads). The RBCM (red), merozoite plasma membrane (cyan), rhoptry organelles (orange) and merozoite nuclear membrane (green) are also highlighted. In the C2-arrested WT schizont, a Maurer's Cleft (MC) is visible within the erythrocyte cytoplasm. Scale bars, 100 nm.

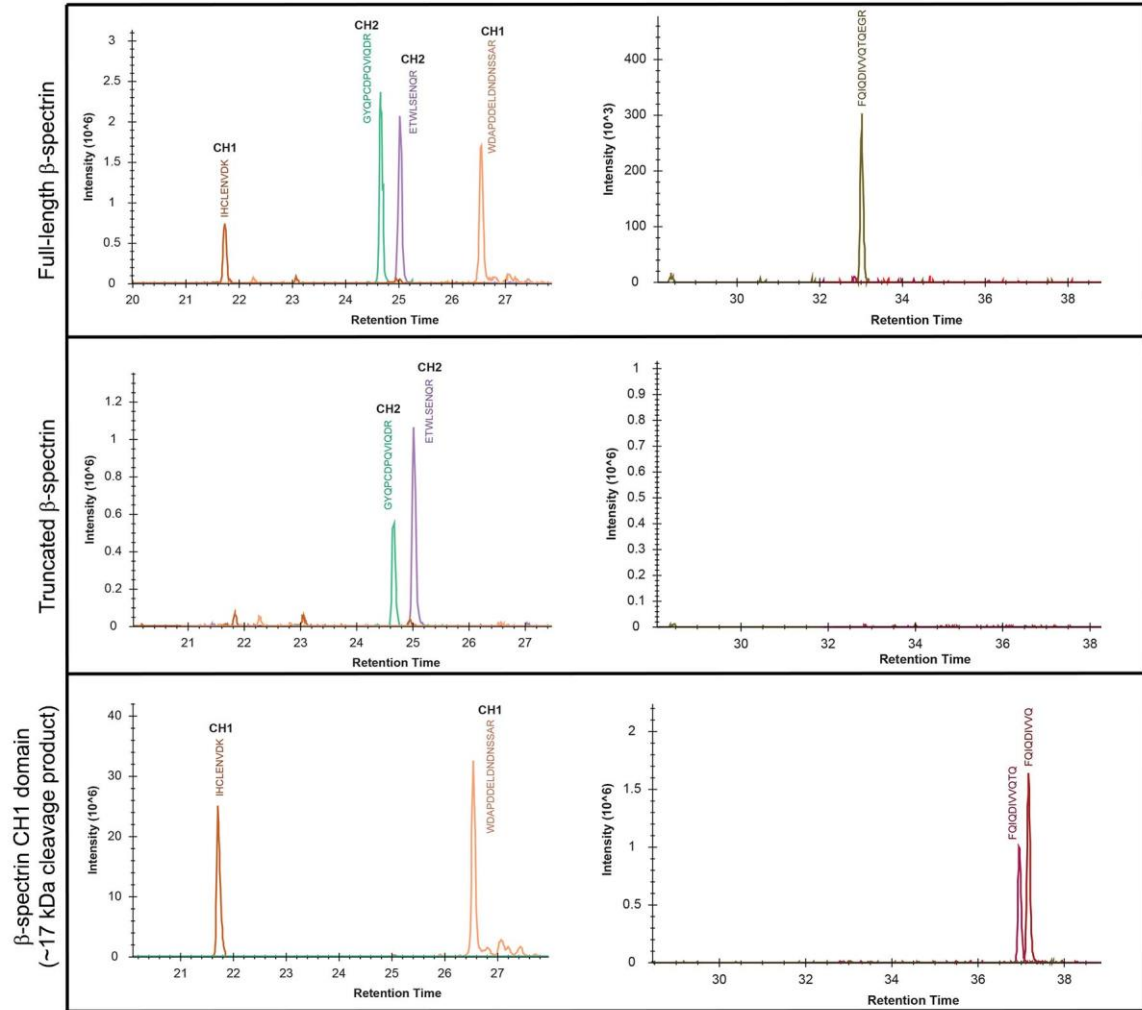
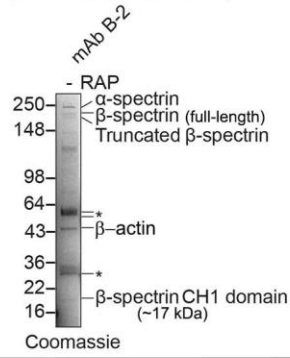


Supplementary Figure 6. Egress is associated with appearance of low molecular mass cleavage product(s) derived from the N-terminal region of β -spectrin. Mock- or RAP-treated *SERA6:loxP* schizonts were incubated for \sim 4 h with C2, then the egress block released by washing and further incubation for 20 minutes in protein-free medium lacking C2. Soluble fractions of the entire preparations were then subjected to SDS PAGE on a 4-12% linear gradient gel, and slices processed for tryptic digestion and LC-MS/MS. Shown are fragmentation spectra of two β -spectrin-derived semi-tryptic peptides that were enriched in the mock-treated sample in digests corresponding to the molecular mass range \sim 15-20 kDa, and so likely form the C-termini of the cleavage product(s). The two peptides overlap by 2 residues, suggesting that cleavage to produce the polypeptide(s) occurs at two closely-spaced sites between Gln167-Glu168 and between Gln165-Thr166. Numbering is based on the complete sequence of human β -spectrin (UniprotKB P11277).



Supplementary Figure 7. RBCM rupture is associated with cleavage of the RBC cytoskeletal protein β -spectrin at 2 closely-spaced sites between the N-terminal CH1 and CH2 domains. Shown are Skyline ion chromatograms of selected β -spectrin peptides identified by LC-MS/MS of tryptic digests of species present in pull-downs shown in [Fig. 4d](#) of the main manuscript (a relevant section of the gel is shown; the Coomassie-stained profile is representative of 4 completely independent pull-down experiments in which the results were fully reproducible). Left, Digests of full-length β -spectrin were found to contain peptides from both CH1 and CH2 domains, as expected. In contrast, digests of the truncated high molecular mass β -spectrin cleavage product contained CH2 domain peptides but not CH1 domain peptides, indicating loss of its N-terminal segment, whilst digests of the \sim 17 kDa cleavage product contained only CH1 domain peptides, showing it represents an N-terminal fragment. Right, ion chromatograms of peptides 157FQIQDIVVQTQEGR170, 157FQIQDIVVQTQ167, and 157FQIQDIVVQ165, which lie between the CH1 and the CH2 domains (numbering based on the complete sequence of human β -spectrin; UniprotKB P11277). Tryptic peptide 157FQIQDIVVQTQEGR170 was present in digests of full length β -spectrin but absent from both high and low molecular mass cleavage products, consistent with proteolytic processing occurring within this sequence. Semi-tryptic peptides 157FQIQDIVVQTQ167 and 157FQIQDIVVQ165 were detected only in digests of the \sim 17 kDa fragment (see also [Supplementary Fig. 6](#)) indicating that they represent its C-terminus.

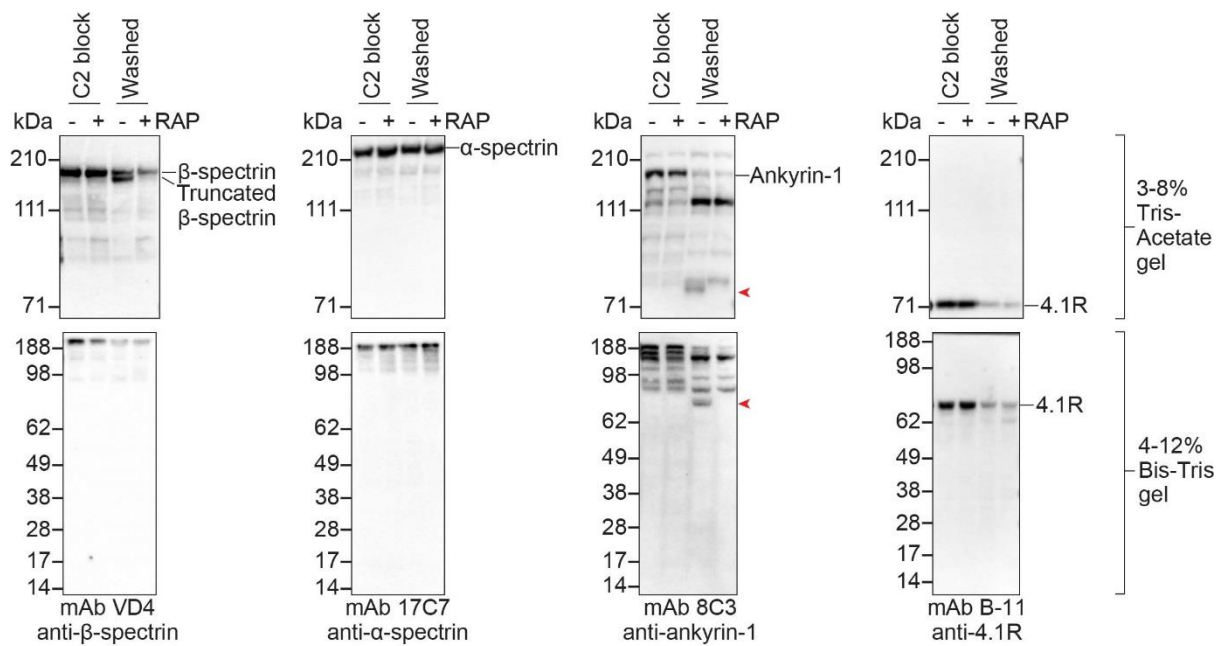
mAb used for pull-down



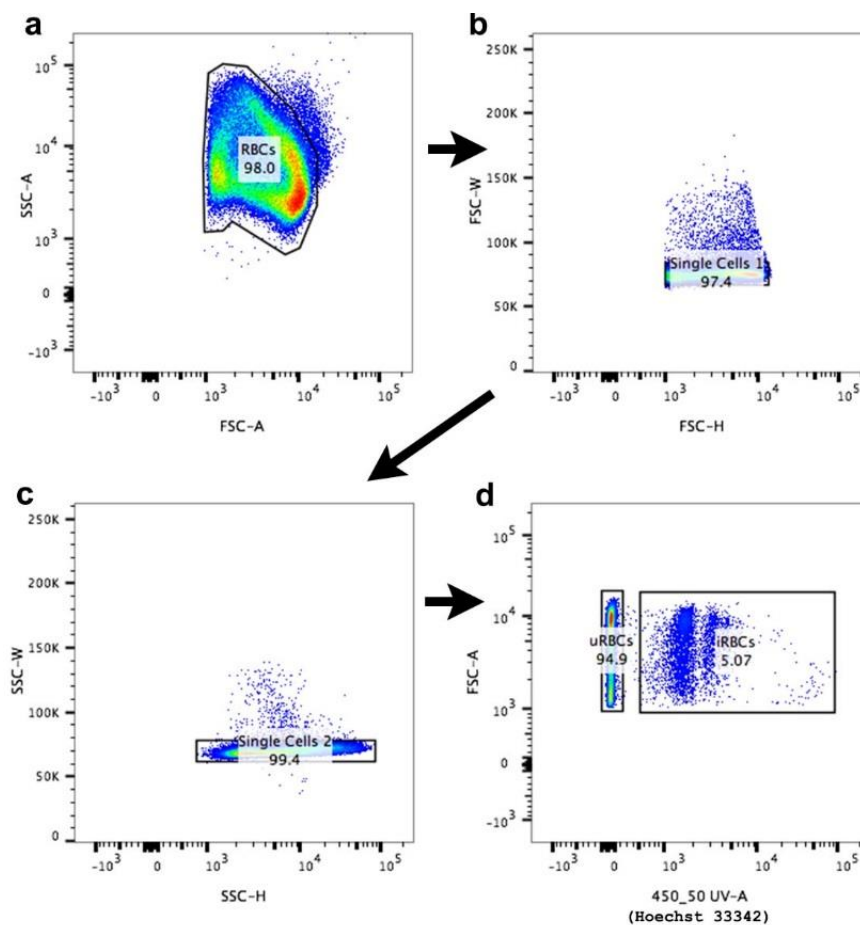
Supplementary Figure 8. Human β -actin co-purifies with the cleaved ~17 kDa CH1 domain of β -spectrin. Peptide coverage obtained by LC-MS/MS analysis of tryptic digests of the ~45 kDa co-precipitating protein present in pull-downs performed with anti- β -spectrin mAb B-2 from soluble extracts of mock-treated *SERA6:loxP* schizonts allowed to proceed to egress for just 20 minutes (see Fig. 4d of the main manuscript). Identified sequences are highlighted in bold red text and comprise 58% coverage, unambiguously identifying the protein as human β -actin (UniProtKB P60709).

1	MDDDI AALVV	DNGSGMCKAG	FAGDDAPRAV	FPSIVGRPRH	QGV M VGMGQK
51	DSYVGDEAQS	KRGILTLKYP	IEHGIVTNWD	DMEKIWHHTF	YNELR V A P E E
101	HPVLLTEAPL	NPK ANREKMT	QIMFETFNTP	AMYVAIQAVL	SLYASGR T T G
151	IVMDSGDGVT	HTVPIYEGYA	LPHAILRLDL	AGR DLTDYLM	KIL TER GYSF
201	TTTAEREIVR	DIKE KLCYVA	LDFEQEMATA	ASSSLEKSY	ELPDGQVITI
251	GNERFRCPEA	LFQPSFLGME	SCGIHETTFN	SIMK CDVDIR	KDLYANTVLS
301	GGTTMYPGIA	DRMQKEITAL	APSTMKIKII	APPERKYSVW	IGGSILASLS
351	TFQQMWISK Q	EYDESGPSIV	HRKCF		

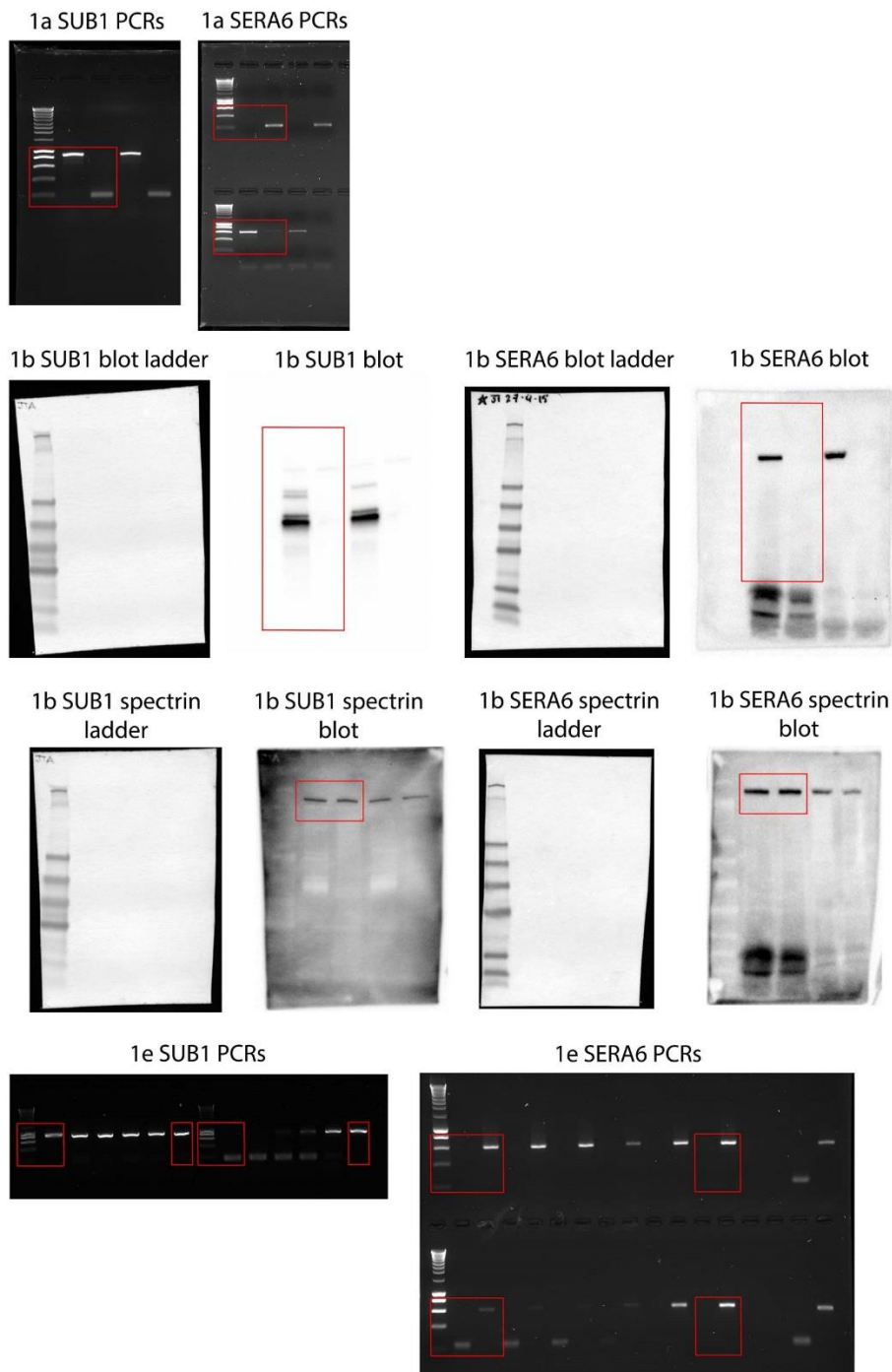
Supplementary Figure 9. The RBC cytoskeletal protein ankyrin undergoes limited SERA6-dependent proteolysis at egress. Western blots showing analysis of compound 2 (C2)-arrested *SERA6:loxP* schizonts or parallel cultures extracted just 20 minutes following washing away the C2 in order to allow progress to egress. The parasite extracts were probed with the indicated monoclonal antibodies (mAbs). Egress-associated truncation of β -spectrin was readily detectable in the control (-RAP) *SERA6:loxP* schizonts that were allowed to proceed to egress, and limited cleavage of ankyrin was also noted (cleavage products indicated with red arrowheads). However, no SERA6-dependent cleavage of the other cytoskeletal components α -spectrin or protein 4.1R was observed. Each Western was performed using two different SDS PAGE gel systems in order to aid detection of both high and low molecular mass proteins. The data shown are representative of 2 fully independent experiments with identical results.



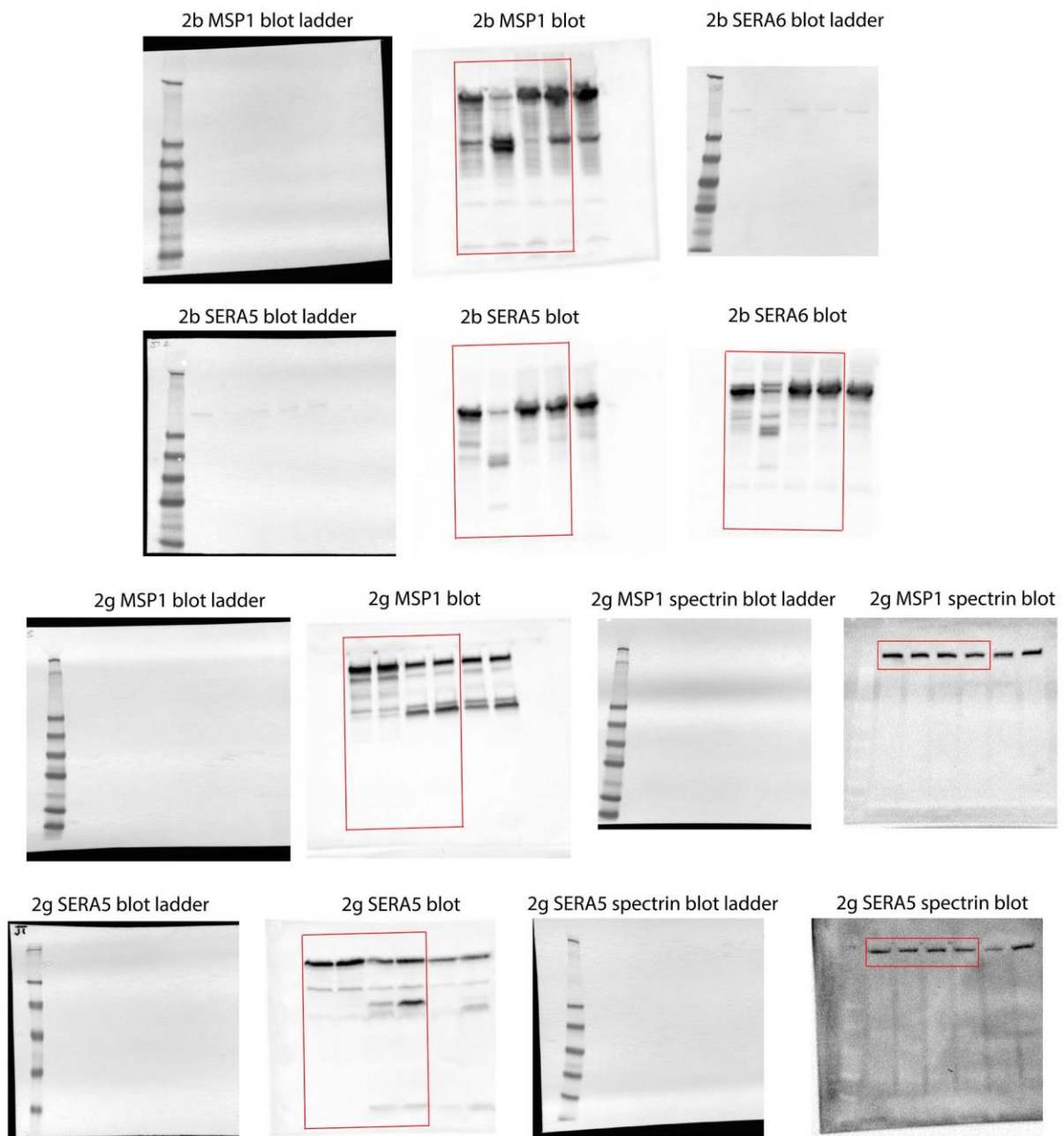
Supplementary Figure 10. Gating strategy for measurement of *P. falciparum* parasitaemia levels by flow cytometry (FACS). This method relies on the fact that uninfected mature erythrocytes do not possess a nucleus and so do not label with the DNA stain Hoechst 33342. Parasitised cells, in contrast, stain strongly. **a**, Cells to be counted were initially screened using forward (FSC-A) and side scatter (SSC-A) areas to gate for all erythrocytes. **b**, The selected population was subsequently gated to remove doublets (adherent cell clusters) by gating on plots of forward scatter width (FSC-W) against forward scatter height (FSC-H). **c**, A second round of doublet discrimination was then performed by gating on plots of side scatter width (SSC-W) and side scatter height (SSC-H). **d**, Finally, parasite-infected erythrocytes (iRBCs) were gated as positive for the DNA stain by plotting forward scatter area (FSC-A) against 450_50 UV-A fluorescence. Note that the iRBCs fall into populations with distinct levels of staining intensity depending on the extent to which nuclear division has taken place. In this case the great majority were ring-stage (mononuclear). uRBCs, uninfected erythrocytes. In each dot plot, figures refer to the fraction (percentage) of the total displayed population within each gated area.



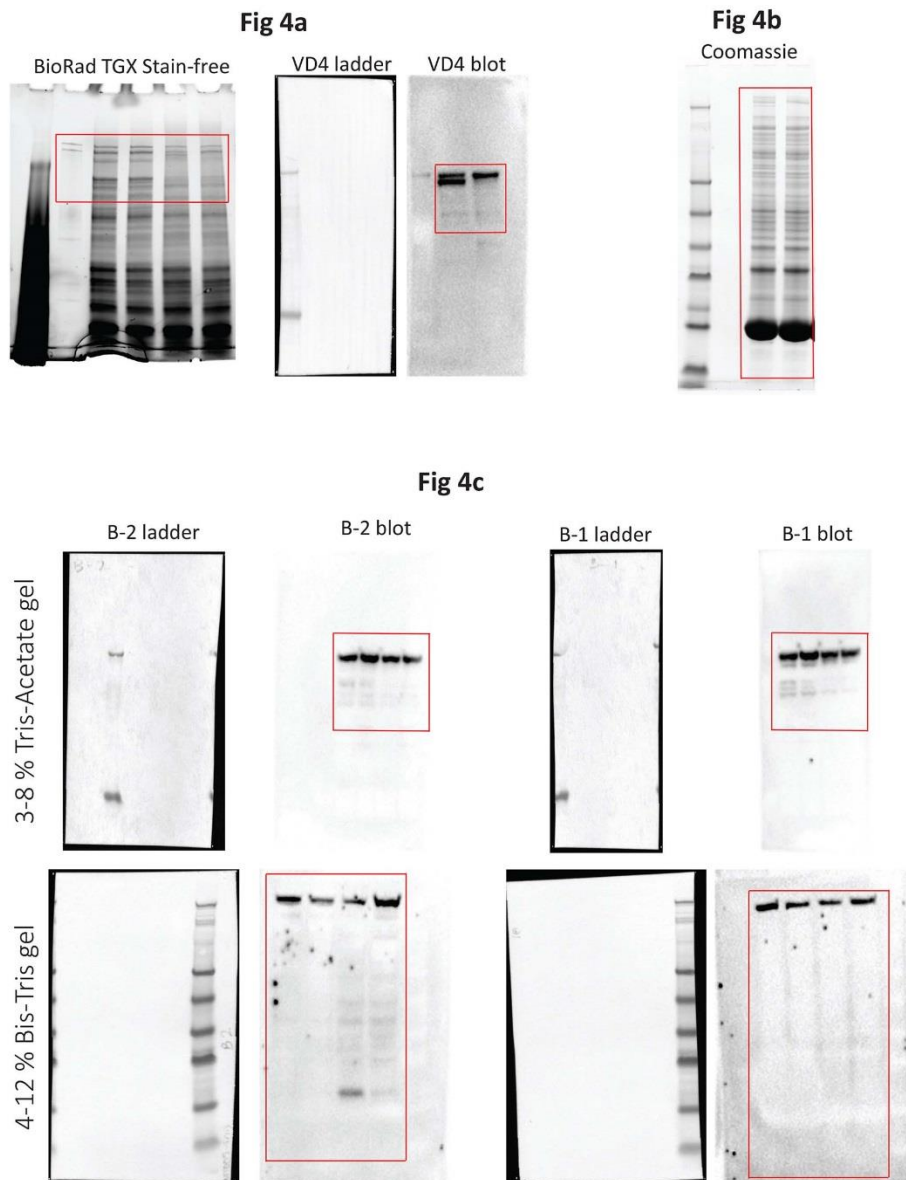
Supplementary Figure 11. Unedited full-length gels/blots used in main text figures. Shown are unmanipulated (raw) versions of the images shown in Figure 1a, 1b, and 1e; The images have been edited only to include boxes (red) that highlight which parts of the full gels/blots are reproduced in the corresponding figures. Note that the pre-stained molecular weight markers (ladder) were imaged separately from the corresponding chemiluminescent Western blot images, and so are displayed separately.



Supplementary Figure 12. Unedited full-length blots used in main text figures. Shown are unmanipulated (raw) versions of the images shown in Figure 2b and 2g; The images have been edited only to include boxes (red) that highlight which parts of the full gels/blots are reproduced in the corresponding figures. Note that the pre-stained molecular weight markers (ladder) were imaged separately from the corresponding chemiluminescent Western blot images, and so are displayed separately.

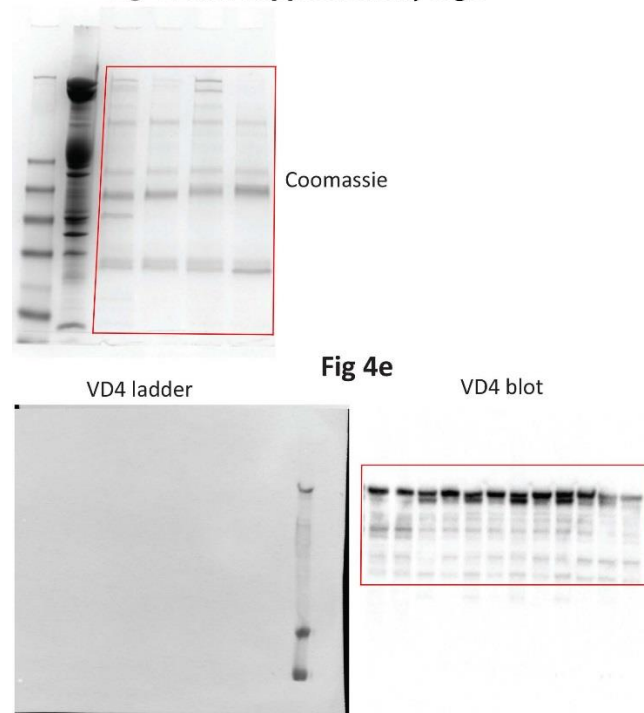


Supplementary Figure 13. Unedited full-length gels/blots used in main text. Shown are unmanipulated (raw) versions of the images shown in Figure 4a-c. The images have been edited only to include boxes (red) that highlight which parts of the full gels/blots are reproduced in the corresponding figures. Note that the pre-stained molecular weight markers (ladder) were imaged separately from the corresponding chemiluminescent Western blot images, and so are displayed separately.

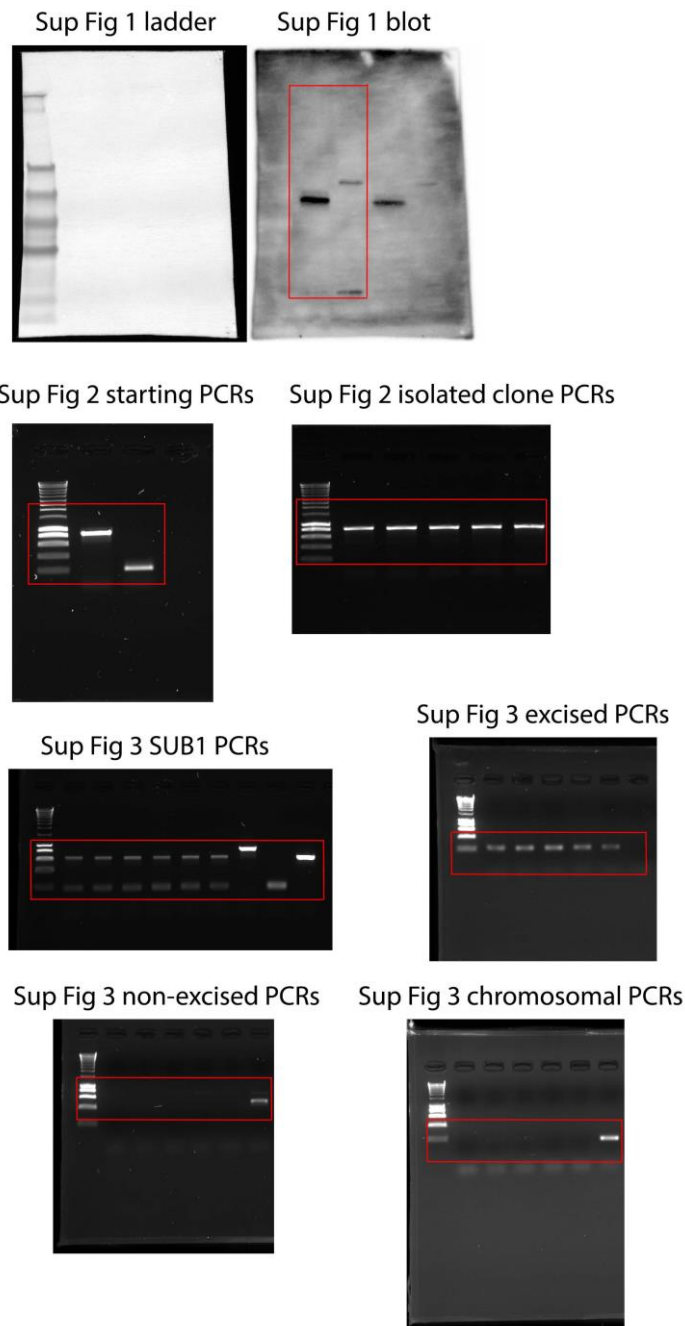


Supplementary Figure 14. Unedited full-length gels/blots used in main text and Supplementary figures. Shown are unmanipulated (raw) versions of the images shown in Figure 4d-e and Supplementary Figure 7 (top). The images have been edited only to include boxes (red) that highlight which parts of the full gels/blots are reproduced in the corresponding figures. Note that the pre-stained molecular weight markers (ladder) were imaged separately from the corresponding chemiluminescent Western blot images, and so are displayed separately.

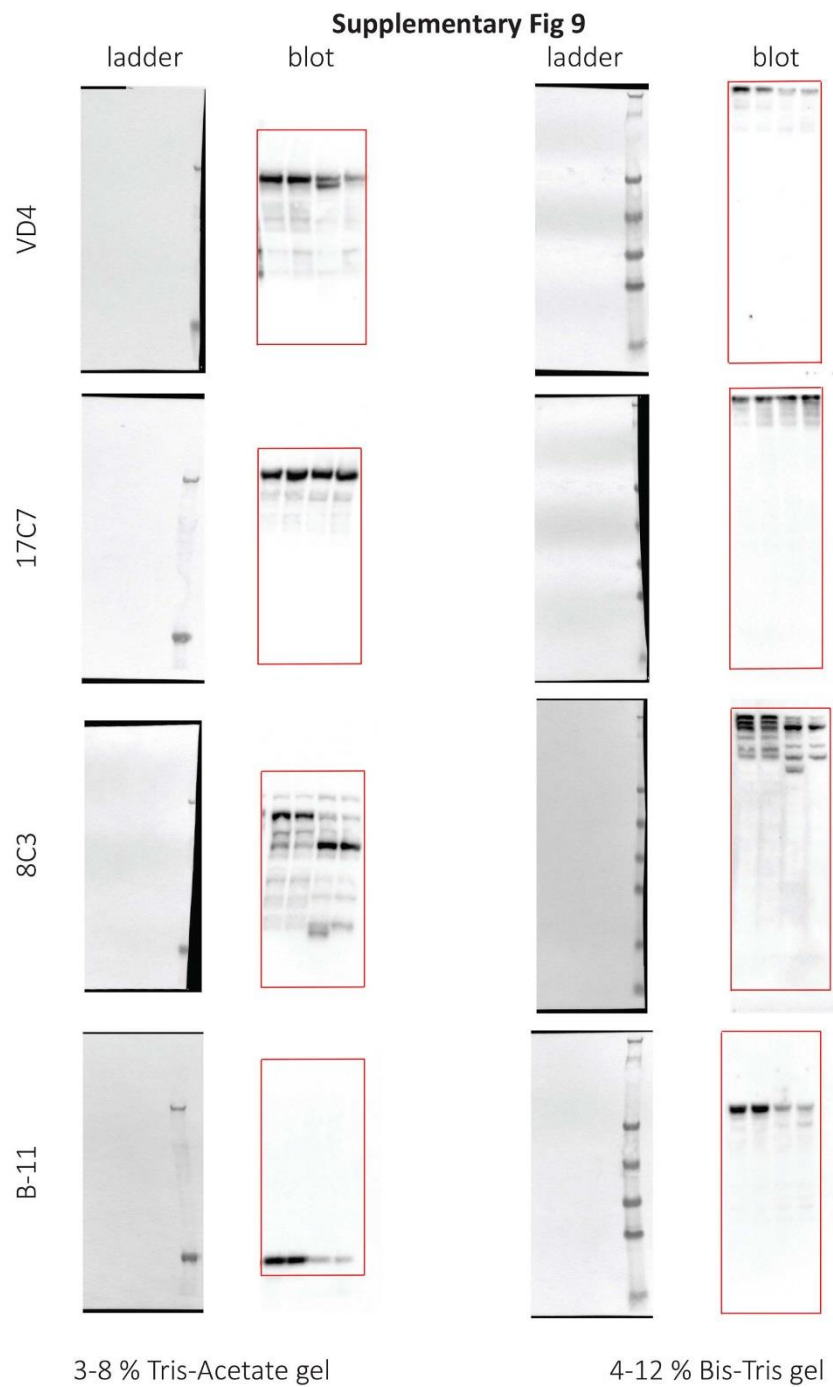
Fig 4d and Supplementary Fig 7



Supplementary Figure 15. Unedited full-length gels/blots used in Supplementary figures. Shown are unmanipulated (raw) versions of the images shown in Supplementary Figures 1, 2 and 3. The images have been edited only to include boxes (red) that highlight which parts of the full gels/blots are reproduced in the corresponding figures. Note that the pre-stained molecular weight markers (ladder) were imaged separately from the corresponding chemiluminescent Western blot images, and so are displayed separately



Supplementary Figure 16. Unedited full-length gels/blots used in Supplementary figures. Shown are unmanipulated (raw) versions of the images shown in Supplementary Figure 9. The images have been edited only to include boxes (red) that highlight which parts of the full gels/blots are reproduced in the corresponding figures. Note that the pre-stained molecular weight markers (ladder) were imaged separately from the corresponding chemiluminescent Western blot images, and so are displayed separately.



Supplementary Table 1. Oligonucleotide primers used in this study.

Primer name	Primer sequence (5' – 3')
SERA6-34 (4 ^a)	GTCCTGGAAGAAGAACGTTGCCGCCGAGACACAACACTGACTTCATG
S65'UTRb-2	CAGAAAAAGTAAAAGACCAAATGATA
S6EndoEx2Rev	CTTCAGAACATTTATTTTGAAGTTCC
SERA6-37	AAGTAGGAGTCGGACTTAGAA
JTS5synthF (3 ^a)	GAATGCTATTTCTGCTACGTG
JTPbDT3'R (2 ^a)	TTACAGTTATAAATACAATCAATTGG
JT111-6p (1 ^a)	GAGTACCTGCAAAGAAAGGGTATCTTG
hsp863'R1 (5 ^a)	GACTTTACTGAGACATG
JTPrA1 (6 ^a)	GGTTACGGGATCATGTGGG
S6synthRev2 (7 ^a)	GTTCAAAACGTTGTGAGTGATG
JT-S1CO-F	GAATATAGTGGTATTTTTAATTCTTCTGTGCGAGTACCTGCAAAGAAAGGG
JT-S1synth-R	AGTCTAACTAGTCTCGAGGTGCAGGTATCTGGACTTCTTCTT
JT-S1endo-F	TAAGTTCCATGGGTAAACAACATAGGAGGGAATGAGGTAGATGC
JT-S1CO-R	CCCTTTCTTTCAGGTACTIONCGACAGAAGAATTAATAAATACCACTATATTC
S65'UTRb-2	CAGAAAAAGTAAAAGACCAAATGATA
S6EndoEx2Rev	CTTCAGAACATTTATTTTGAAGTTCC
SERA6-5'UTRb	AAAAGTAAAAGACCAAATGATA
SERA6-37	AAGTAGGAGTCGGACTTAGAA
JT111-1p	GATTGTTAGCGAATTACGATTCCTAG
JT111-2p	GAACAGTTCGACGCAGACACGAAGAAC
JT111-3p	GATGACTACAATTACTTGCAGATAC
PfSUB1-synth-for-infu	CGGCTAGCCGATTACTGCATGGCCATATAAATGTTACAAATTC
PfSUB1-synth-rev-infu	GGCATCTACCTCATTCCCTCCTATG
PbDT3UTR-for_infu	GAGGGATATGGCAGCTTAATGTTC
PbDT3UTR-rev_infu	CCCCCGGGTCGATACGCCTACCCTGAAGAAGAAAAGTCC

^aNumerical codes as used in [Fig. 1](#) of the main manuscript as well as [Supplementary Fig. 2](#) and [Supplementary Fig. 3](#).

Supplementary References

- 1 Blackman, M. J. *et al.* A subtilisin-like protein in secretory organelles of *Plasmodium falciparum* merozoites. *J Biol Chem* **273**, 23398-23409 (1998).
- 2 Sajid, M., Withers-Martinez, C. & Blackman, M. J. Maturation and specificity of *Plasmodium falciparum* subtilisin-like protease-1, a malaria merozoite subtilisin-like serine protease. *J Biol Chem* **275**, 631-641 (2000).